Ran Ran, Cui-E Hu*, Yan Cheng*, Xiang-Rong Chen and Guang-Fu Ji

First-principles study of structures, elastic and optical properties of single-layer metal iodides under strain

https://doi.org/10.1515/zna-2020-0157
Received June 13, 2020; accepted August 5, 2020; published online September 7, 2020

Abstract: The structure, elastic, electronic and optical properties of two-dimensional (2D) MI_2 (M = Pb, Ge, Cd) under strain are systematically studied by the first-principles method. It is proved that the monolayer structure of 2D-MI_2 is stable by phonon spectra. Moreover, the large ideal strain strength (40%), the large range of strain and the elastic constants of far smaller than other 2D materials indicate that the single-layer PbI_2 and GeI_2 possess excellent ductility and flexibility. By applying appropriate strain to the structure of 2D-MI_2, the band gaps of single-layer MI_2 can be effectively controlled (PbI_2: 1.04 ~ 3.03 eV, GeI_2: 0.43 ~ 2.99 eV and CdI_2: 0.54 ~ 3.36 eV). It is found that the wavelength range of light absorbed by these three metal iodides is 82–621 nm, so 2D-MI_2 has great absorption intensity for ultraviolet light in a large wavelength range, and the strain of structure can effectively regulate the optical parameters.

Keywords: elastic properties; first-principles; metal iodide (MI_2); optical properties.

1 Introduction

For two-dimensional (2D) materials, the movement of electrons is limited in the plane, so they have some physical and chemical properties that block materials do not have. These unique properties make 2D materials develop rapidly. With the development of graphene, boron nitride (h-BN), transition metal sulfides (TMDs), monoene, transition metal carbides, transition metal oxides and other 2D materials, some drawbacks have gradually emerged [1–9], such as the band gap loss of graphene, the low carrier concentration of TMDs and so on. In order to meet the specific needs of production, some new 2D materials, such as metal iodide, have been explored [10–13].

For single-layer metal iodides (MI_2), the most representative materials are 2D lead iodide (2D-PbI_2), germanium iodide (2D-GeI_2) and cadmium iodide (2D-CdI_2). There are many kinds of phase, among which the most stable is 2H phase, which is a sandwich structure stacked in the ABC model [14]. The layer of MI_2 where the metal atom M is located is sandwiched between two I layers, and there is a van der Waals force between the layers [15]. Stable structure, band gap comparable to third-generation semiconductors, excellent physical and chemical properties are the characteristics of metal iodides. Single-layer PbI_2 can be used to make radiation-proof devices because of its high atomic number and density [16–18]; single-layer GeI_2 has a unique light absorption range and can be used to prepare photoelectric converter devices [19, 20]; single-layer CdI_2 is a good material for making heterojunction and heterojunction arrays [21, 22]. According to previous reports, the single-layer metal iodide MI_2 (M = Pb, Ge, Cd) has been successfully stripped and grown in the laboratory.

There are many methods to obtain single-layer MI_2, including mechanical peeling, solution method and physical vapour deposition [23]. Most single-layer structures can be obtained by mechanical peeling, but the production efficiency of this method is relatively low. The sample prepared by this method has small transverse size and poor thickness control, so it is impossible to prepare a large area of single-layer structure. Impurities are easily introduced in the preparation of monolayer structures using solution method, thus affecting the properties. In contrast, the yield of vapour deposition method is higher and the quality of single-layer structure produced is better [24]. Monolayer structure of metal iodides has been prepared on a large scale in experiments, but the number of layers, phases, densities of defects and edge morphology of samples is uncertain due to limitations of experimental equipment. The physical properties of 2D metal iodides cannot be accurately studied. Therefore, the theoretical calculation of single-layer metal iodides is very necessary.

***Corresponding authors: Cui-E Hu**, College of Physics and Electronic Engineering, Chongqing Normal University, Chongqing 400047, China, E-mail: cuiehu@126.com; and **Yan Cheng**, College of Physics, Sichuan University, Chengdu 610064, China, E-mail: ycheng@scu.edu.cn
Ran Ran and Xiang-Rong Chen, College of Physics, Sichuan University, Chengdu 610064, China
Guang-Fu Ji, Institute of Fluid Physics, Chinese Academy of Engineering Physics, Mianyang 621900, China

In 2015, Zhou et al. [25] explored the structure, stability, electronic and optical properties of single-layer PbI_2 and showed some significant results. In our previous work, the single-layer structure, electronic, elastic and thermal transport properties of PbI_2 have been explored and some important results have been obtained [26]. However, previous studies have been limited to PbI_2, which is not representative and does not take into account the properties under strain.

In this work, the structure, elastic and optical properties of single-layer metal iodide MI_2 (M = Pb, Ge, Cd) under strain are first investigated by using the first-principles method. Firstly, it is proved that the monolayer structure of MI_2 is stable by the phonon spectra. Then, the stress-strain curve, elastic constant, Young's modulus, layer modulus and Poisson's ratio of 2D-MI_2 are obtained. Comparing with other 2D materials, it can be concluded that 2D-MI_2 has excellent flexibility and ductility, as well as good ability to adjust strain. Considering the spin–orbit coupling (SOC) effect, the band structure and optical parameters in the strain ranging from −20 to 20% were calculated by using the hybrid functional Heyd-Scuseria-Ernzerhof (HSE06). Our results show that the strain can effectively regulate the band gap and optical absorption properties of 2D-MI_2.

2 Theoretical methods and calculation details

The Vienna Ab initio Simulation Package (VASP) based on first-principles is applied to all our calculations [27–29]. The Perdew-Burke-Ernzerhof method in the generalized gradient approximation model is used in the structural optimization and elastic calculations [30, 31]. For the calculation of electronic structure, we use the hybrid functional (HSE06) approximation and consider the influence of SOC [32–34]. After the convergence tests, the plane wave cut-off energies were set to 440, 500 and 400 eV for single-layer PbI_2, GeI_2 and CdI_2, respectively. The forces on all relaxed atoms were less than 10^{-4} eV/Å, and the energy convergence criterion was 10^{-6} eV per unit cell. The k-point sampling grids in the Brillouin zone were chosen as $15 \times 15 \times 1$ for geometry optimization and $21 \times 21 \times 1$ for the calculation of elastic properties.

In general, the elastic constants of materials are derived from the relationship between stress and strain. The relationship between stress and strain can be expressed as follows [35]:

$$\sigma_{ij} = C_{ijkl}\,\varepsilon_{kl} \tag{1}$$

The metal iodide studied in this paper belongs to hexagonal system, so there are only six independent elastic constants.

$$C_{\text{hexal}} = \begin{pmatrix} C_{11} & C_{12} & C_{13} & & & \\ \cdot & C_{11} & C_{13} & & & \\ \cdot & \cdot & C_{33} & & & \\ & & & C_{44} & & \\ & & & & C_{44} & \\ & & & & & C_{66} \end{pmatrix} \tag{2}$$

In fact, there are only five independent elastic constants because for the hexagonal structure C_{66} is obtained from C_{11} and C_{12} ($C_{66} = (C_{11} - C_{12})/2$) [36]. The above elastic theory can also be applied to 2D materials, but some details are different. Different from bulk material, the strain of 2D material is in plane. We know that bulk modulus represents the resistance of bulk materials to external forces. Similarly, the ability of 2D materials to resist external forces (in-plane) can be expressed by layer modulus γ [36], which is given as follows:

$$\gamma = -A\frac{\partial F}{\partial A} = A\frac{\partial}{\partial A}\left(\frac{\partial E}{\partial A}\right) = A\frac{\partial^2 E}{\partial A^2} \tag{3}$$

In addition, some other parameters which can be used to express the elastic properties of 2D materials can also be calculated by elastic constants. Young's modulus Y and Poisson's ratio v can be expressed as follows [36]:

$$Y^{2D}_{[10]} = \frac{C_{11}C_{12} - C_{12}^2}{C_{22}} \tag{4}$$

$$Y^{2D}_{[01]} = \frac{C_{11}C_{12} - C_{12}^2}{C_{11}} \tag{5}$$

$$v^{2D}_{[10]} = \frac{C_{12}}{C_{22}} \tag{6}$$

$$v^{2D}_{[01]} = \frac{C_{12}}{C_{11}} \tag{7}$$

The optical properties of materials are represented by some optical parameters, such as reflectivity, refractive index, absorption coefficient, energy loss and so on. The interaction between light and the electrons and atoms it passes through produces light absorption, which reveals the optical properties of materials and also contains the information of electronic structure. To explore the optical properties of materials, we need to calculate the complex dielectric function, which is expressed as follows [37]:

$$\varepsilon(\omega) = \varepsilon_1(\omega) + i\varepsilon_2(\omega) \tag{8}$$

The imaginary part of the complex dielectric function ε_2 can be obtained by the sum of occupied and unoccupied wave functions, as follows [37]:

$$\varepsilon_{\alpha\beta}(\omega) = \frac{4\pi^2 e^2}{\Omega} \lim_{q\to 0} \frac{1}{q^2} \sum_{c,v,k} 2w_k \delta(\varepsilon_{ck} - \varepsilon_{vk} - \varepsilon) \times \langle u_{ck+e_\alpha q} | u_{vk} \rangle \langle u_{ck+e_\beta q} | u_{vk} \rangle^* \tag{9}$$

Among them, $e_x\,(x = \alpha, \beta, \gamma)$ represents the unit vector in Cartesian direction, u_k represents the periodic part of the primitive cell of pseudo wave function, c and v are the conduction band and the valence band, respectively. The real part of the complex dielectric function ε_1 can be deduced by Kramer-Kronig relation on the basis of the imaginary part, as follows [38]:

$$\varepsilon_1(\omega) = 1 + \frac{2}{\pi} P \int \frac{\omega' \varepsilon_2(\omega')}{\omega'^2 - \omega^2} d\omega' \tag{10}$$

Then, the reflectivity and absorption coefficient can be obtained by the following formula [38]:

$$R(\omega) = \left| \frac{\sqrt{\varepsilon_1(\omega) + j\varepsilon_2(\omega)} - 1}{\sqrt{\varepsilon_1(\omega) + j\varepsilon_2(\omega)} + 1} \right|^2 \tag{11}$$

$$\alpha = \sqrt{2\left[-\varepsilon_1(\omega) \pm \sqrt{\varepsilon_1^2(\omega) + \varepsilon_2^2(\omega)} \right]} \tag{12}$$

3 Results and discussion

3.1 Structure and elasticity

The most stable phase of bulk MI_2 (M = Pb, Ge, Cd) is the semiconducting 2H phase, whose unit cell consists of two iodide atoms and a metal atom. Figure 1a shows the bulk structure. Recleave surface was performed to achieve a monolayer crystal structure, that is, the bulk phase of MI_2 was cleaved along (0 0 1) plane. After convergence test, we found that the vacuum layer of 8 Å is enough when eliminating the interaction between layers from Figure 1b. In addition, the lattice constants, bond lengths and bond angles of the optimized monolayer MI_2 are shown in Table 1. Our previous work has proved the stability of single-layer PbI_2 [26]. It can be seen in Figure 2 that all phonon modes in monolayer MI_2 have positive frequency indicating the stability of this structure.

After the stable single-layer structure is obtained, the strain-stress curve is calculated to explore the ability of 2D-MI_2 to resist external strain. Figure 3 depicts the stress per unit length ($N{\cdot}m^{-1}$) as a function of strain (%). It can be seen from Figure 3 that the strain-stress curves of single-layer PbI_2 and GeI_2 are relatively similar. The maximum stresses are 10.6 and 12.11 $N{\cdot}m^{-1}$, respectively, and the corresponding ideal strains are all around 40%, indicating that their structures can stretch to 40% of the original. The stress-strain curve of CdI_2 is different from those of PbI_2 and GeI_2. Its maximum stress is 18.81 $N{\cdot}m^{-1}$, and the corresponding ideal strain is 24%, which is obviously lower than the former two. Compared with the ideal strain strength of other 2D materials, such as MoS_2 (20%) and graphene (24%) [39–42], the ideal strain strength of single-layer PbI_2 and GeI_2 as high as 40% makes them show excellent strain capacity and flexibility. On the one hand, this is due to their fold structures. For example, the surfaces of graphene and h-BN are flat, and there are no folds in z direction; some 2D materials have fold structures but close to plane structures. These 2D materials have no space to coordinate the strain when they are stressed, either they have high hardness and are not easy to deform or they have general hardness and their structures are easily damaged. What is more is that this phenomenon can also be explained by elasticity theory.

As it is known, another parameter that can indicate the resistance to compression is the elastic constant.

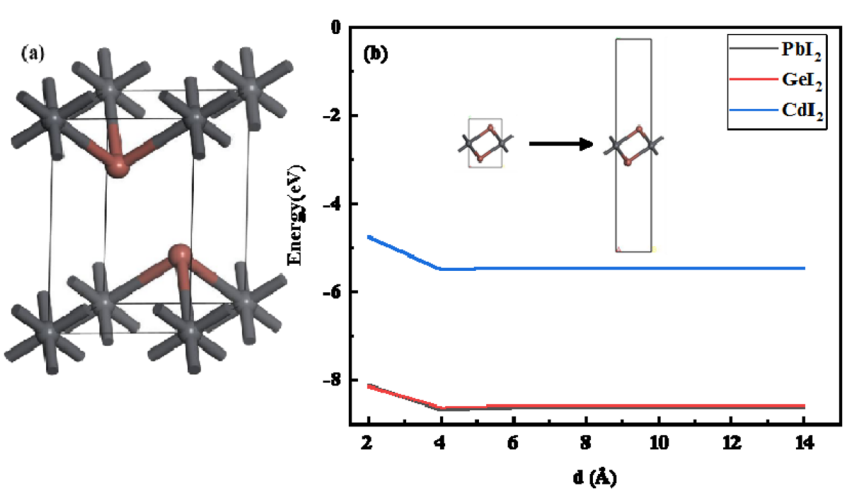

Figure 1: (Colour online) (a) Unit cell of 2H-metal iodide. Grey and red balls represent metal atoms and I atoms, respectively; (b) The energy dependences of the height of the vacuum layer.

Table 1: The lattice constants, I–M bond lengths and M–I–M bond angles of monolayer MI_2 (M = Pb, Ge, Cd).

	Single-layer PbI_2	Single-layer GeI_2	Single-layer CdI_2
Lattice constants (Å)	4.66	4.30	4.34
I–M bond lengths (Å)	3.23	3.04	3.04
M–I–M bond angles	89.84°	90.31°	91.10°

The value of elastic constant (C_{11}), Young's modulus (Y^{2D}) and shear modulus (G^{2D}) is listed in Table 2. Compared with other 2D materials, the Young's modulus of 2D-MI_2 (M = Pb, Ge, Cd) is far lower than that of *h*-BN (289 N·m^{-1}), 2D TMDs like MoS_2 (199 N·m^{-1}), WS_2 (272 N·m^{-1}) and TcS_2 (93 N·m^{-1}) but similar to that of phosphorene (armchair) (44 N·m^{-1}) [36, 43–45]. Therefore, the 2D-MI_2, which is more flexible, also has potential applications in flexible optoelectronics. Nevertheless, although both single-layer PbI_2 and GeI_2 are metal iodides, the Young's modulus of PbI_2 is nearly 40% smaller than that of GeI_2. To further explore why single-layer PbI_2 is more flexible, the Bader charge analysis has be done. The I–M bond is a transitional form between the covalent bond and ionic bond. In general, the stronger the ionicity, the weaker the resistance of the chemical bond to an external force and therefore the smaller the elastic constant. Each I atom gets 0.45 e transferred from the Pb atom when Pb atom is bonding with I atom, but instead, each I atom gets 0.36 e transferred from the Ge atom when Ge atom is bonding with I atom. So single-layer PbI_2 is more ionic, which leads to a smaller Young's modulus. What is more is that it can be seen from Table 2 that the ratio of layer modulus and sheer modulus (γ/G^{2D}) of GeI_2 is less than 1.75, indicating its brittleness [46], whereas that of MI_2 (M = Pb, Cd) is greater than 1.75, showing good ductility.

By summarizing the above calculation, it can be concluded that 2D-MI_2 has low hardness, excellent flexibility and the ability to coordinate strain, so it can be utilized to synthesize some semiconductor devices that require extensive strain.

Table 2: Calculated elastic constants (C_{11} and C_{12} in N·m^{-1}), sheer modulus (G^{2D} in N·m^{-1}), Young's modulus (Y^{2D} in N·m^{-1}) and layer modulus (γ in N·m^{-1}).

	C_{11}	C_{12}	G^{2D}	Y^{2D}	γ	γ/G^{2D}
Monolayer PbI_2	14.69	3.95	5.30	13.63	9.35	1.80
Monolayer GeI_2	23.76	5.36	9.20	22.55	14.56	1.58
Monolayer CdI_2	22.85	8.26	7.29	19.86	15.56	2.13

3.2 Electronic structure

Materials will be deformed due to the action of external forces in the process of practical application, so it is meaningful to explore the change of electronic structure in the case of strain. The electronic structure of monolayer PbI_2 and GeI_2 under strain is systematically studied in this section. Firstly, the strain structure is optimized, and then, the electronic structure is calculated. All kinds of lattice

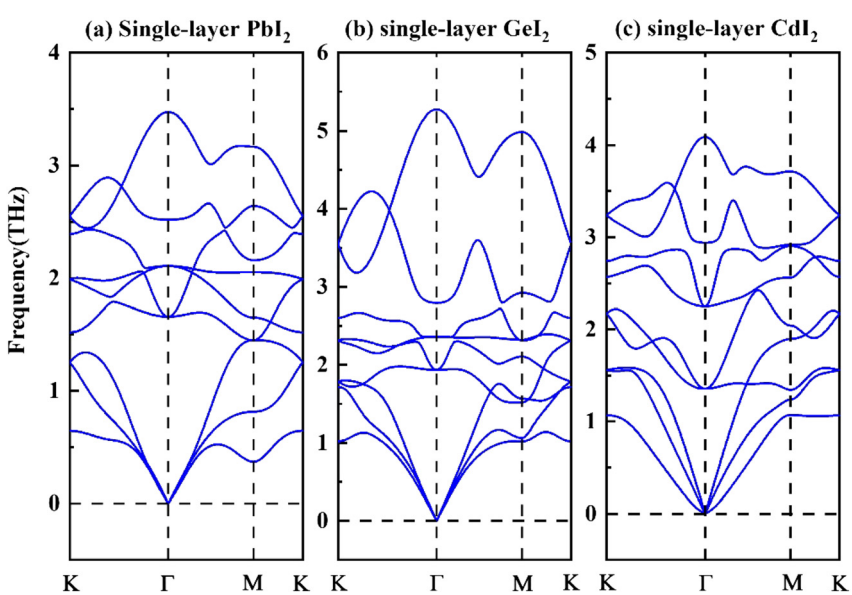

Figure 2: (Colour online) The phonon spectra of (a) 2D-PbI_2 [26], (b) 2D-GeI_2 and (c) 2D-CdI_2.

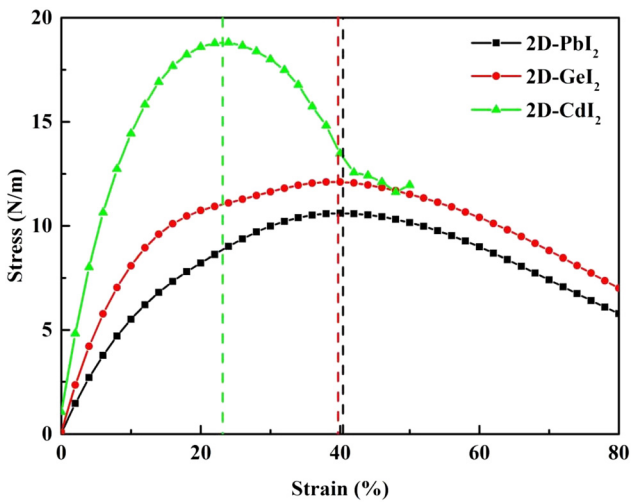

Figure 3: (Colour online) The stress-strain curves for single-layer MI_2 (M = Pb, Ge, Cd).

parameters along lattice vector of a/b direction are chosen. A biaxial strain is defined as $\varepsilon = \Delta a/a_0$, where Δa is the difference between the frozen and optimized lattice constant along lattice vector a/b direction and a_0 is the equilibrium lattice constant.

The electronic structure of single-layer MI_2 (M = Pb, Ge, Cd) under different strain is shown in Figure 4a–c. In the calculation process, the top of valence band is Fermi surface. It can be clearly seen that the conduction band of single-layer PbI_2 decreases continuously and the valence band increases continuously with the stretching of the structure. In this process, the position of the bottom of the conduction band is always at the Γ-point, but the position of the top of the valence band changes from the position between Γ-point and M-point in equilibrium state to the position of M-point (the ε is more than 15%). For single-layer GeI_2, the variation trend of its valence band and conduction band is basically the same as that of single-layer PbI_2. The only difference is the position of the conduction band bottom when $\varepsilon = -10\%$. The change of electronic structure of CdI_2 under strain is different from that of PbI_2 and GeI_2. With the compression of the structure, the bottom of the conduction band decreases gradually. In this process, the position of the bottom of the conduction band and the top of the valence band has not changed. When the structure is stretched, the conduction band rises slowly to $\varepsilon = 5\%$ and then drops sharply. At the same time, the position of the bottom of the conduction band changes from M-point ($\varepsilon = 0 \sim 5\%$) to Γ-point ($\varepsilon > 10\%$), and the position of the top of the valence band changes from Γ-point to the position between Γ-point and M-point. The band gap of single-layer MI_2 is always indirect, no matter in tension or compression.

The curve of band gap calculated by the HSE06 + SOC method with strain is shown in Figure 5. It can be seen that the band gaps of single-layer PbI_2 and single-layer GeI_2 continue to increase with the compression strain of the structures. When they increase to 3.03 and 2.89 eV (compression strain to –10%), respectively, the band gap drops sharply. As the tensile strain of the structure goes on, the band gap decreases. The curve of single-layer CdI_2 is different from the former two. With the compression of the structure, the band gap of the single-layer CdI_2 decreases gradually. With the structure stretching, the band gap increases slowly at first and suddenly drops sharply when it increases to 3.46 eV (tensile strain is around 5%).

Through the above analysis, we can conclude that compared with compression strain, stretching can regulate the band gap of single-layer CdI_2 more efficiently, while single-layer PbI_2 and GeI_2 are the opposite, because compression has a more significant role in regulating the band gap of both. In addition, in the process of strain changing from –20 to 20%, the effect of strain on the band gap of single-layer MI_2 is very obvious (CdI_2: 0.54 ~ 3.46 eV, PbI_2: 1.04 ~ 3.03 eV, GeI_2: 0.43 ~ 2.99 eV). Therefore, the structural strain can effectively control the band gap of single-layer MI_2. In the application, the appropriate strain can be applied to the single-layer MI_2 to obtain the desired band gap so that it can be used in the photoelectric devices that need specific band gap.

3.3 Optical properties

Now, we calculate the optical properties of the monolayer metal iodide MI_2 (M = Pb, Ge, Cd). We first calculate the real part ε_1 and the imaginary part ε_2 of the dielectric function. Then, we use Eqs. (8) and (9) to get the absorption curve and reflection curve. The real part ε_1 and imaginary part ε_2 of dielectric function, absorption coefficient, reflectivity of the single-layer MI_2 as a function of photon energy are shown in Figure 6. It can be seen from Figure 6a and b that the real part and imaginary part of 2D-MI_2 have a maximum value in the low energy region (infrared, visible and near ultraviolet). Clearly, we can see from Figure 6c that PbI_2 and GeI_2 monolayers have two similar absorption bands. The absorption curve of single-layer CdI_2 is different from that of single-layer PbI_2 and GeI_2, which is due to the fact that Cd atom is not in the same group as Pb and Ge atoms. For single-layer PbI_2, GeI_2 and CdI_2, the absorptions begin when the photon energy is zero, and the energies at the absorption edge are basically consistent with the corresponding band gaps.

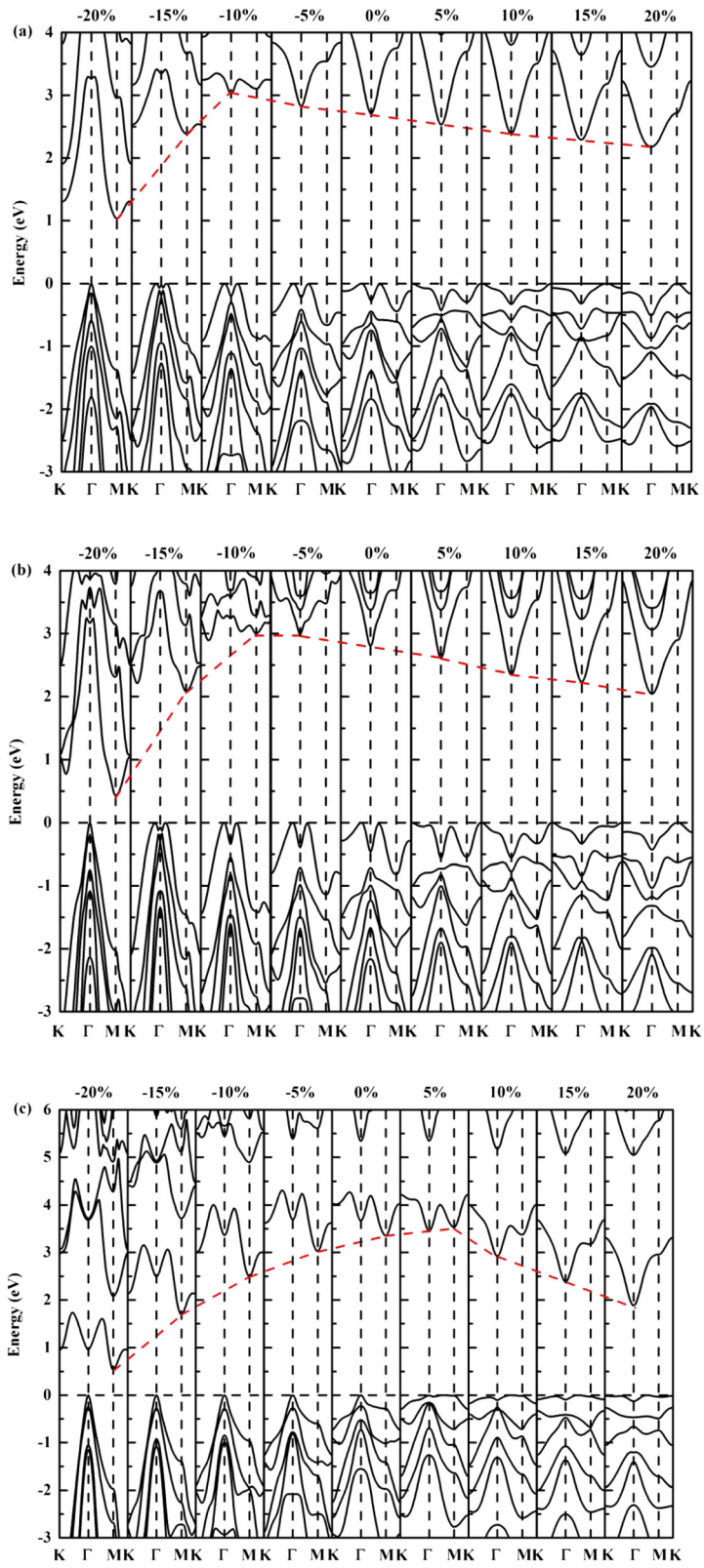

Figure 4: (Colour online) The electronic structure of single-layer MI_2 (M = Pb, Ge, Cd) under different strains.

However, it can be found that the energy at the absorption edge is slightly lower than that in the band gap because the energy required for free carrier absorption is lower than that for the intrinsic absorption, and free carrier absorption occurs when the energy is lower than the forbidden band energy. With the increase of photon

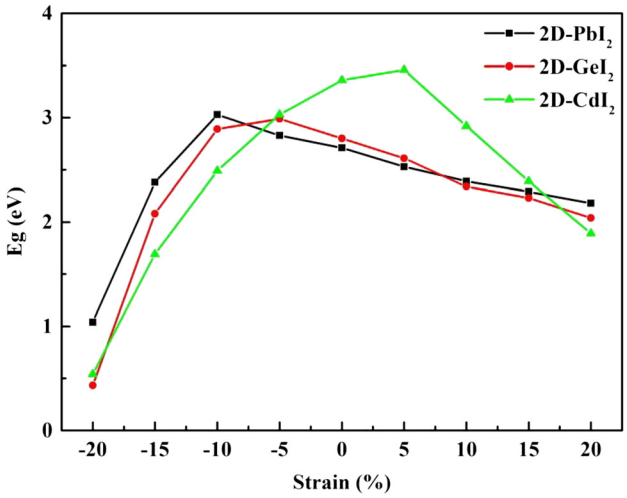

Figure 5: (Colour online) The curves of band gaps of single-layer MI_2 (M = Pb, Ge, Cd) calculated by the HSE06 + SOC method.

energy, the ε_2 of MI_2 rises rapidly in the visible light region and then the peak appears, indicating the absorption part of the visible light. The first peak appeared in the absorption spectrum of MI_2 near 4 eV, and the light absorption of single-layer PbI_2 and GeI_2 reached 790,000 cm^{-1} and 750,000 cm^{-1}, respectively, indicating that the single-layer PbI_2 and GeI_2 have a strong absorption capacity for ultraviolet light, while CdI_2 has relatively weak absorption capacity for UV light. However, the absorption spectrum of single-layer MI_2 in the range of UV light appears several peaks continuously, and the peak value is also very large. To sum up, we can conclude that the monolayer MI_2 has a strong absorption capacity for ultraviolet light in a wide range of wavelengths. It can be seen from Figure 6d that the first peak appears in the visible light region for the reflection, and then many peaks appear in the ultraviolet light region, with the highest reflectivity around 50, 47 and 34% for single-layer PbI_2, GeI_2 and CdI_2, respectively. In general, there are many peaks in the reflection curve of single-layer MI_2, which are concentrated in the UV region, and the peak value is small, showing that the main reflective parts of the 2D-MI_2 are visible light and ultraviolet light, but the reflectivity is not high. However, they have strong absorption capacity for UV light and can be used to make UV detection devices or anti-UV radiation devices.

In view of the strong ability of 2D-MI_2 to absorb UV light in the equilibrium state, the optical absorption

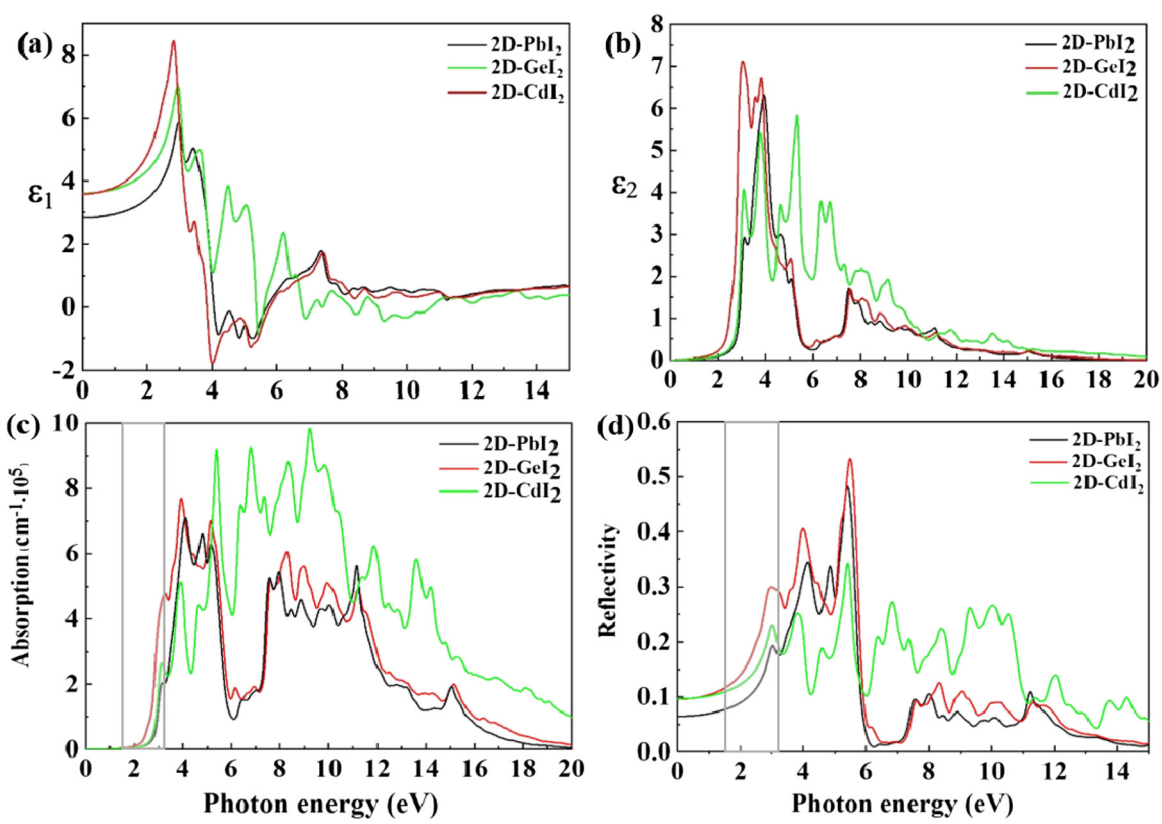

Figure 6: (Colour online) (a) The real part ε_1 and (b) imaginary part ε_2 of dielectric function, (c) absorption coefficient, (d) reflectivity of single-layer MI_2 (M = Pb, Ge, Cd) as a function of photon energy.

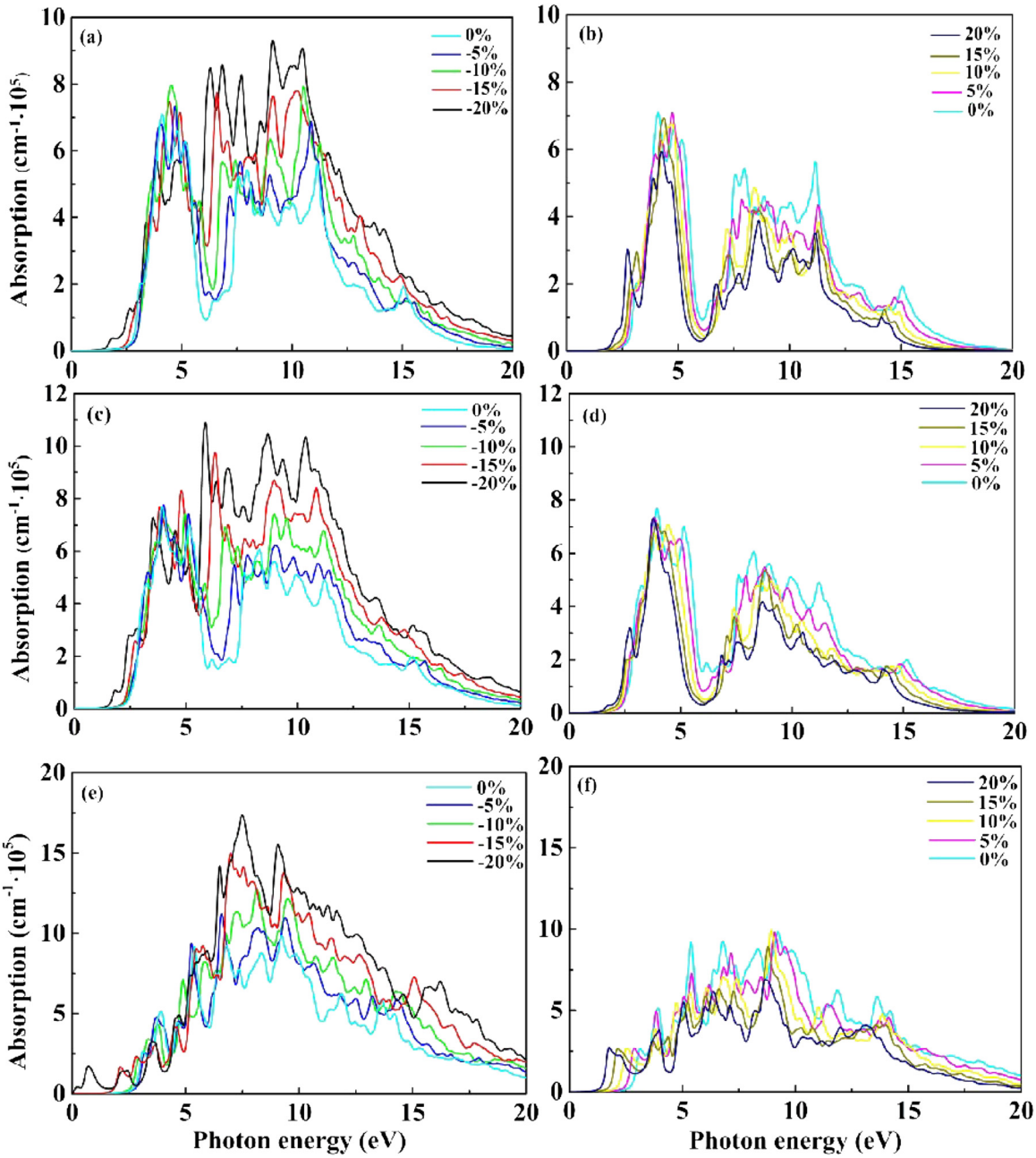

Figure 7: (Colour online) Absorption spectra of 2D-PbI_2 (a, b), 2D-GeI_2 (c, d) and 2D-CdI_2 (e, f) under compressions (–20 ~ 0%) and tensions (0 ~ 20%).

properties of single-layer MI_2 under strains are further calculated, and the results are shown in Figure 7. Among them, Figure 7 (a), (c) and (e) show the absorption spectra of singe-layer PbI_2, GeI_2 and CdI_2 under compressions ($\varepsilon = -20 \sim 0\%$), respectively, while (b), (d) and (f) show the absorption spectra of the three under tensions ($\varepsilon = 0 \sim 20\%$). It can be seen that the light absorptions still start at 0 eV even though the structures are strained. When the structure is compressed, the absorption edge value moves to the left, while the absorption edge value moves to the right when the structure is stretched. This is due to the change of band gap. The absorption band of 2D-MI_2 becomes narrower and lower with the tensile strain. On the other hand, the compressive strain can improve the optical absorption of 2D-MI_2 expanding the range of absorbing ultraviolet. Therefore, the strain can effectively regulate the light absorption ability of single-layer MI_2 so that it can be used in different photoelectric detection devices.

4 Conclusions

The structural, elastic and optical properties of 2D metal iodide MI_2 (M = Pb, Ge, Cd) in equilibrium and strain are systematically studied by using the first-principles method. It is proved that the monolayer structure of MI_2 (M = Pb, Ge, Cd) is stable, and it presents a fold structure similar to "sandwich". Because of this fold structure, single-layer PbI_2 and GeI_2 have large ideal strain strength (40%), indicating that they have a good strain capacity and excellent flexibility. In addition, the layer modulus γ, Young's modulus Y^{2D}, Poisson's ratio v and shear modulus G^{2D} are calculated. The results show that the layer modulus of single-layer MI_2 is much smaller than other two-dimensional materials, showing the characteristics of small hardness and good flexibility. The excellent flexibility, ductility and strong ability of coordinating strain all make the 2D-MI_2 be used to manufacture photoelectric devices with large strain range.

The effect of strain on the band of 2D-MI_2 was investigated using the HSE06 + SOC method. It is found that the effect of structural compression on the band gap of single-layer PbI_2 and GeI_2 is more significant, but structural stretching can change the band gap of single-layer CdI_2 more efficiently. From $\varepsilon = -20\%$ to $\varepsilon = 20\%$, the change of the band gap of single-layer MI_2 is very obvious (CdI_2: 0.54 ~ 3.46 eV; PbI_2: 1.04 ~ 3.03 eV; GeI_2:0.43 ~ 2.99 eV). Therefore, the strain can effectively control the band gap of single-layer MI_2. By exploring the optical properties, it is found that the single-layer MI_2 has strong absorption ability for ultraviolet light over a large wavelength range. Moreover, strain can not only effectively change the band gap but also effectively control the light absorption ability.

Acknowledgments: This work was supported by the NSAF Joint Fund Jointly setup by the National Natural Science Foundation of China and the Chinese Academy of Engineering Physics (Grant No. U1830101) and the Science Challenge Project (Grant No. TZ2016001).

Author contribution: All the authors have accepted responsibility for the entire content of this submitted manuscript and approved submission.

Research funding: This work was supported by the NSAF Joint Fund Jointly setup by the National Natural Science Foundation of China and the Chinese Academy of Engineering Physics (Grant No. U1830101) and the Science Challenge Project (Grant No. TZ2016001).

Conflict of interest statement: The authors declare no conflicts of interest regarding this article.

References

[1] K. S. Novoselov, A. K. Geim, S. V. Morozov et al., "Electric field effect in atomically thin carbon films," *Science*, vol. 306, pp. 666–669, 2004.
[2] A. K. Geim and K. S. Novoselov, "The rise of graphene," *Nat. Mater.*, vol. 6, pp. 183–191, 2007.
[3] T. Ouyang, Y. P. Chen, Y. Xie, K. K. Yang, Z. G. Bao, and J. X. Zhong, "Thermal transport in hexagonal boron nitride nanoribbons," *Nanotechnology*, vol. 21, p. 245701, 2010.
[4] Q. Peng, W. Ji, and S. De, "Mechanical properties of the hexagonal boron nitride monolayer: Ab initio study," *Comput. Mater. Sci.*, vol. 56, pp. 11–17, 2012.
[5] X. Hou, Z. Xie, C. Li, G. Li, and Z. Chen, "Study of electronic structure, thermal conductivity, elastic and optical properties of alpha, beta, gamma-graphyne," *Materials*, vol. 11, p. 188, 2018.
[6] B. Radisavljevic, A. Radenovic, J. Brivio, V. Giacometti, and A. Kis, "Single-layer MoS_2 transistors," *Nat. Nanotechnol.*, vol. 6, pp. 147–150, 2011.
[7] T. Cheiwchanchamnangij and W. R. L. Lambrecht, "Quasiparticle band structure calculation of monolayer, bilayer, and bulk MoS_2," *Phys. Rev. B*, vol. 85, p. 205302, 2012.
[8] H. Li, Q. Zhang, C. C. R. Yap et al., "From bulk to monolayer MoS_2: Evolution of Raman scattering," *Adv. Funct. Mater.*, vol. 22, pp. 1385–1390, 2012.
[9] S. Sahoo, A. P. S. Gaur, M. Ahmadi, M. J. F. Guinel, and R. S. Katiyar, "Temperature-dependent Raman studies and thermal conductivity of few-layer MoS_2," *J. Phys. Chem. C*, vol. 117, pp. 9042–9047, 2013.
[10] H. Liu, A. T. Neal, Z. Zhu, et al., "Phosphorene: An unexplored 2D semiconductor with a high hole mobility," *ACS Nano*, vol. 8, pp. 4033–4041, 2014.
[11] B. Jhun and C. S. Park, "Electronic structure of charged bilayer and trilayer phosphorene," *Phys. Rev. B*, vol. 96, p. 085412, 2017.
[12] S. Manzeli, D. Ovchinnikov, D. Pasquier, O. V. Yazyev, and A. Kis, "2D transition metal dichalcogenides," *Nat. Rev. Mater.*, vol. 2, p. 17033, 2017.
[13] Y. Jiao, F. Ma, G. Gao, J. Bell, T. Frauenheim, and A. Du, "Versatile single-layer sodium phosphidostannate(II): Strain-tunable electronic structure, excellent mechanical flexibility, and an ideal gap for photovoltaics," *J. Phys. Chem. Lett.*, vol. 6, pp. 2682–2687, 2015.
[14] B. Palosz, "The structure of PbI_2 polytypes 2H and 4H: A study of the 2H–4H transition," *J Phys. Matter.*, vol. 2, pp. 5285–5295, 1990.
[15] R. Ahuja, H. Arwin, A. F. D. Silva et al., "Electronic and optical properties of lead iodide," *J. Appl. Phys.*, vol. 92, pp. 7219–7224, 2002.
[16] C. Shen, and G. Wang, "Electronic and optical properties of bilayer PbI_2: A first-principles study," *J Phys. D*, vol. 51, p. 035301, 2018.
[17] P. H Wangyang, H. Sun, X. H. Zhu, D. Y. Yang, and X. Y. Gao, "Mechanical exfoliation and Raman spectra of ultrathin PbI_2 single crystal," *Mater. Lett.*, vol. 168, pp. 68–71, 2016.
[18] J. C. Lund, K. S. Shah, M. R. Squillante, L. P. Moy, F. Sinclair, and G. Entine, "Properties of lead iodide semiconductor radiation detectors," *Nucl. Instrum. Methods Phys. Res. Sect. A Accel. Spectrom. Detect. Assoc. Equip.*, vol. 283, pp. 299–302, 1989.

[19] C. S. Liu, X. L. Yang, J. Liu, and X. J. Ye, "Exfoliated monolayer GeI_2: Theoretical prediction of a wide-band gap semiconductor with tunable half-metallic ferromagnetism," *J. Phys. Chem. C*, vol. 122, pp. 22137–22142, 2018.
[20] E. Urgiles, P. Melo, and C. C. Coleman, "Vapor reaction growth of single crystal GeI_2," *J. Cryst. Growth*, vol. 165, pp. 245–249, 1996.
[21] S. Bellucci, I. Bolesta, M. C. Guidi et al., "Cadmium clusters in CdI_2 layered crystals: The influence on the optical properties," *J. Phys. Condens. Matter*, vol. 19, p. 395015, 2007.
[22] R. D. Singh, A. Gaur, A. K. Sharma, and N. V. Unnikrishnan, "Multiphoton photoconductivity in an indirect band gap crystal: CdI_2," *Solid State Commun.*, vol. 72, pp. 595–598, 1989.
[23] Y. G. Wang, L. Gan, J. N. Chen, R. Yang, and T. Y. Zhai, "Achieving highly uniform two-dimensional PbI_2 flakes for photodetectors via space confined physical vapor deposition," *Sci. Bull.*, vol. 62, pp. 1654–1662, 2017.
[24] M. Z. Zhong, S. Zhang, L. Huang et al., "Large-scale 2D PbI_2 monolayers: Experimental realization and their indirect band-gap related properties," *Nanoscale*, vol. 9, pp. 3736–3741, 2017.
[25] M. Zhou, W. H. Duan, Y. Chen, and A. J. Du, "Single layer lead iodide: Computational exploration of structural, electronic and optical properties, strain induced band modulation and the role of spin–orbital-coupling," *Nanoscale*, vol. 7, pp. 15168–15174, 2015.
[26] R. Ran, C. Cheng, Z. Y. Zeng, X. R. Chen, and Q. F. Chen, "Mechanical and thermal transport properties of monolayer PbI_2 via first-principles investigations," *Philos. Mag. A*, vol. 99, pp. 1277–1296, 2019.
[27] G. Kresse and J. Furthmuller, "Efficiency of ab-initio total energy calculations for metals and semiconductors using a plane-wave basis set," *Comput. Mater. Sci.*, vol. 6, pp. 15–50, 1996.
[28] G. Kresse and D. Joubert, "From ultrasoft pseudopotentials to the projector augmented-wave method," *Phys. Rev. B*, vol. 59, pp. 1758–1775, 1999.
[29] K. Yabana and G. F. Bertsch, "Time-dependent local-density approximation in real time," *Phys. Rev. B*, vol. 54, pp. 4484–4487, 1996.
[30] J. P. Perdew, K. Burke, and M. Ernzerhof, "Generalized gradient approximation made simple," *Phys. Rev. Lett.*, vol. 77, pp. 3865–3868, 1996.
[31] M. E. Casida, C. Jamorski, K. C. Casida, and D. R. Salahub, "Molecular excitation energies to high-lying bound states from time-dependent density-functional response theory: Characterization and correction of the time-dependent local density approximation ionization threshold," *J. Chem. Phys.*, vol. 108, pp. 4439–4449, 1998.
[32] J. Heyd, G. E. Scuseria, and M. Ernzerhof, "Hybrid functionals based on a screened Coulomb potential," *J. Chem. Phys.*, vol. 118, pp. 8207–8215, 2003.
[33] C. M. Marian, "Spin–orbit coupling and intersystem crossing in molecules," *WIREs Comput. Mol. Sci.*, vol. 2, pp. 187–203, 2012.
[34] Y. K. Kato, R. C. Myers, A. C. Gossard, and D. D. Awschalom, "Observation of the spin hall effect in semiconductors," *Science*, vol. 306, pp. 1910–1913, 2004.
[35] F. Mouhat and F. Coudert, "Necessary and sufficient elastic stability conditions in various crystal systems," *Phys. Rev. B*, vol. 90, p. 224104, 2014.
[36] R. C. Andrew, R. E. Mapasha, A. M. Ukpong, and N. Chetty, "Mechanical properties of graphene and boronitrene," *Phys. Rev. B*, vol. 85, p. 125428, 2012.
[37] H. R. Philipp and H. Ehrenreich, "Optical properties of semiconductors," *Phys. Rev.*, vol. 129, pp. 1550–1560, 1963.
[38] K. R. Waters, M. S. Hughes, G. H. Brandenburger, and J. G. Miller, "On a time-domain representation of the Kramers–Krönig dispersion relations," *J. Acoust. Soc. Am.*, vol. 108, pp. 2114–2119, 2000.
[39] C. G. Andres, R. Roldán, E. Cappelluti et al., "Local strain engineering in atomically thin MoS_2," *Nano Lett.*, vol. 13, pp. 5361–5366, 2013.
[40] C. Li, B. Fan, W. Li et al., "Bandgap engineering of monolayer MoS_2 under strain: A DFT study," *J Korean Phys. Soc.*, vol. 66, pp. 1789–1793, 2015.
[41] M. H. Cha, J. Hwang, J. Ihm, and K. S. Kim, "Ideal strength of graphene under general states of tensile strain," *Bull. Am. Phys. Soc.*, vol. 59, no. 1, 2014, https://meetings.aps.org/link/BAPS.2014.MAR.C1.13.
[42] Z. Ni, T. Yu, Y. Lu, Y. Wang, Y. P. Feng, and Z. Shen, "Uniaxial strain on graphene: Raman spectroscopy study and band-gap opening," *ACS Nano*, vol. 2, pp. 2301–2305, 2008.
[43] X. D. Wei, B. Fragneaud, C. A. Marianetti, and J. W. Kysar, "Nonlinear elastic behavior of graphene: Ab initio calculations to continuum description," *Phys. Rev. B*, vol. 80, p. 205407, 2009.
[44] H. L. Zhang and R. Wang, "The stability and the nonlinear elasticity of 2D hexagonal structures of Si and Ge from first-principles calculations," *Physica B*, vol. 406, p. 4080, 2011.
[45] Q. Y. Zhao, Y. H. Guo, Y. X. Zhou et al., "Flexible and anisotropic properties of monolayer MX_2 (M = Tc and Re; X = S, Se)," *J. Phys. Chem. C*, vol. 121, pp. 23744–23751, 2017.
[46] S. F. Pugh, "Relations between the elastic moduli and the plastic properties of polycrystalline pure metals," *Philos. Mag. J. Sci.*, vol. 45, pp. 823–843, 1954. The London, Edinburgh, and Dublin.